Acid Modification of Georgian Natural Heulandite

Vladimer Tsitsishvili[1,2)], Ketevan Ebralidze[3*)], Nanuli Dolaberidze[4)], Nato Mirdzveli[5)], Manana Nijaradze[6)], Zurab Amiridze[7)], Bela Khutsishvili[8)]

[1)] Georgian National Academy of Sciences, 52, Rustaveli Ave., 0108, Tbilisi, Georgia; email: vladimer.tsitsishvili@tsu.ge; https://orcid.org/0000-0003-2592-0973

[2)] Petre Melikishvili Institute of Physical and Organic Chemistry, I.Javakhishvili Tbilisi State University, 31 A.Politkovskaia Str., 1086 Tbilisi, Georgia; email: vladimer.tsitsishvili@tsu.ge; https://orcid.org/0000-0003-2592-0973

[3*)] Petre Melikishvili Institute of Physical and Organic Chemistry, I.Javakhishvili Tbilisi State University, 31 A.Politkovskaia Str., 1086 Tbilisi, Georgia; email: ketevan.ebralidze@tsu.ge; https://orcid.org/0000-0002-4663-6245

[4)] Petre Melikishvili Institute of Physical and Organic Chemistry, I.Javakhishvili Tbilisi State University, 31 A.Politkovskaia Str., 1086 Tbilisi, Georgia; email: nanuli.dolaberidze@tsu.ge; https://orcid.org/0000-0001-6479-2156

[5)] Petre Melikishvili Institute of Physical and Organic Chemistry, I.Javakhishvili Tbilisi State University, 31 A.Politkovskaia Str., 1086 Tbilisi, Georgia; email: nato.mirdzveli@tsu.ge; https://orcid.org/0000-0002-1755-5024

[6)] Petre Melikishvili Institute of Physical and Organic Chemistry, I.Javakhishvili Tbilisi State University, 31 A.Politkovskaia Str., 1086 Tbilisi, Georgia; email: manana.nijaradze@tsu.ge; https://orcid.org/0000-0003-0882-500X

[7)] Petre Melikishvili Institute of Physical and Organic Chemistry, I.Javakhishvili Tbilisi State University, 31 A.Politkovskaia Str., 1086 Tbilisi, Georgia; email: zurab.amiridze@tsu.ge; https://orcid.org/0000-0002-6875-2773

[8)] Petre Melikishvili Institute of Physical and Organic Chemistry, I.Javakhishvili Tbilisi State University, 31 A.Politkovskaia Str., 1086 Tbilisi, Georgia; email: bela.khutsishvili@tsu.ge; https://orcid.org/0000-0003-3685-9506

http://doi.org/10.29227/IM-2024-01-54

Submission date: *16.2.2023* | Review date: *11.3.2023*

Abstract

Acid treatment is a powerful tool for improving the performance of natural zeolites, and the purpose of our work was to study chemical composition, structure and properties of acid-treated heulandite from the Tedzami-Dzegvi deposit. Samples of heulandite-containing tuff from the Rkoni plot with zeolite phase content up to 90%, consisting of heulandite and chabazite in a ratio of 8:1, and having chemical composition described by empirical formula $|Na_{0.25}K_{0.06}Ca_{0.19}Mg_{0.15})|[AlSi_{3.6}O_{9.2}]\cdot 3H_2O$ *were treated with hydrochloric acid solutions with concentration up to 2.0 N. It was established that acid treatment leads to significant dealumination (the molar ratio of Si/Al increases from 3.6 to 9.5) and decationization (the total charge per aluminium atom decreases from 1 to 0.68), sodium and magnesium are mainly leached, calcium and potassium does not take part in the decationization process. Powder X-ray diffraction patterns show that hydrochloric acid solutions with a concentration up to 2.0 N do not lead to amorphization of the zeolite microporous crystal structure, but can gradually dissolve it. The adsorption of water vapor indicates the availability of micropores for the entry of small polar molecules, benzene adsorption shows a slight increase of hydrophobicity of the surface as a result of acid treatment. Nitrogen adsorption-desorption isotherms show acid-mediated sharp increase of adsorption in micropores and of the surface area, as well as changes in the mesoporous system, leading to the prevalence of pores with a diameter of 3 – 10 nm. The concentration of dilute solutions of hydrochloric acid is determined, which provides availability of micropores for large ions and nonpolar molecules, but at which dealumination is insignificant and ion-exchange capacity remains at a sufficient level. Materials obtained by acid treatment of heulandite can be used as adsorbents, ion exchangers, and carriers of biologically active substances and metal ions.*

Keywords: acid treatment, chemical composition, zeolites, filter materials

Introduction

Natural and synthetic zeolites (microporous crystalline aluminosilicates $M_nSi_xAl_nO_{2(n+x)}\cdot mH_2O$ (M^+ = Na^+, K^+, … $½Ca^{2+}$, $½Mg^{2+}$, …) built from alternating SiO_4 and AlO_4^- tetrahedrons forming open framework uniform structures with cages and channels), are considered the most promising sorbents for decontamination of waste and tap water from various harmful impurities due to their molecular-sieve, sorption and ion-exchanging properties [1-4]. In general, synthetic zeolites are more suitable for sequestering heavy metals in wastewater treatment due to the high uniformity of pore size distribution and the presence of a single compensation cation, while natural varieties, although very attractive from an economic and environmental point of view, show the least sorption of heaviest metals [4]. However, to improve the sorption and ion-exchange properties of natural zeolites in order to expand their application in relation to various kinds of pollutants, various modification methods are used, including acid treatment, which makes it possible to increase the surface area of the adsorbent and the porosity of the original natural zeolites [2-4]. For example, exchangeable cations located in the channels and cavities throughout the zeolite structure sometimes block the channel system, but they can be removed by acid treatment [5]. Acid treatment of zeolites is also considered as a secondary synthesis method [6] for the creation of new materials, although in the case of zeolites with a very aluminum content, such as LTA, it leads to structural degradation due to significant dealumination. The process of acid mediated dealumination is proposed to take place through the extraction of aluminum atoms from the zeolite framework and the generation of a hydroxyl nest. It has been established that hydrochloric and nitric acids are more efficient dealuminating agents than sulfuric and phosphoric acids, not to mention weak

organic acids [7]. The most widely used is hydrochloric acid, its effect on the structure and properties of zeolites, as well as treatment conditions (concentration, temperature, duration) with its help are well known [8-10].

The aim of our work was to study acid mediated changes in structure and properties of heulandite-containing tuff from the Tedzami-Dzegvi deposit (Eastern Georgia), intended to create new bactericidal zeolite filter materials for purification and desinfection of water from various sources.

Materials and Methods

Samples of heulandite-clinoptilolite-containing tuff were collected in the southern section of the Tedzami-Dzegvi deposit, Eastern Georgia. According to the results of recent study [6], the sample contains up to ≈90% of zeolite phase with chemical composition described by empirical formula of dehydrated sample $(Na_{1.96}K_{0.47}Ca_{1.49}Mg_{1.17})[Al_{7.8}Si_{28.2}O_{72}]$, and is a high-silica heulandite (crystal chemical data $|Ca_4(H_2O)_{24}|[Al_8Si_{28}O_{72}]$-**HEU** [11, pp. 156-157]) mixed with chabazite ($|Ca_6(H_2O)_{40}|[Al_{12}Si_{24}O_{72}]$-**CHA** [11, pp. 96-97]) in a ratio of 8:1. Zeolitic tuff was crushed on a standard crusher, fractionated to a particle size of 1-1.4 mm or 14-16 mesh, washed with distilled water to remove clay impurities, and dried at a temperature of 95-100 °C.

Acid treatment of samples was carried out by mixing 10 g of original zeolitic tuff with 100 mL of 0.5, 1.0, and 2.0 N HCl solutions in a shaking water bath (OLS26 Aqua Pro, Grant Instruments, US) operating in linear mode at 75 °C. This temperature was chosen as optimal for reasons of reproducibility of the results (control of temperature constancy throughout the acid treatment), as well as for comparison with the results of published works [9-10]. To achieve maximum effect, acid treatment was carried out in three steps: the first lasted 1 hour, the second – 2 hours, and the third – 3 hours, each step was followed by washing with distilled water until no Cl^- ions were detected in the washing water by using $AgNO_3$ solution. Acid treatment with dilute solutions (0.016-0.32 N) was carried out in one step at room temperature

Chemical composition of collected and modified samples was calculated from the X-ray energy dispersive (XR-ED) spectra obtained from scanning electron microscope JSM-6490LV (Jeol, Japan) equipped with INCA Energy 350 XRED analyzer (Oxford, UK). Powder X-ray diffraction (XRD) patterns were obtained from D8 Endeavor diffractometer (Bruker, Germany) employing the Cu-K_α line ($\lambda = 0.154056$ nm); the samples were scanned in the 2Θ range of 5° to 100° with a 0.02° step at a scanning speed of 1°/min. The adsorption capacity for water and benzene vapors was measured under static conditions at room temperature; the samples weighed on an electronic analytical balance (FA 2204N, JOAN LAB, China) were placed in a desiccator and kept for 96 hours at a constant pressure of water vapor (relative pressure p/p_o=0.4 and saturated vapor pressure p/p_o=1.0) and benzene (p/p_o=1.0) and then the samples that absorbed the vapors were weighed again. Nitrogen adsorption/desorption isotherms were measured at 77 K using ASAP 2020 Plus analyzer (Micromeritics, USA) using Brunauer–Emmett–Teller (BET) and Barrett-Joyner-Halenda (BJH) models for data analysis.

Results and Discussions

Changes in the chemical composition of the acid-treated samples indicate their dealumination and decationization; structural changes are fixed by powder X-ray diffraction (XRD) patterns; sorption properties carry information about micro- and mesoporous systems.

Chemical Composition

According to the data of XR-ED spectral analysis, the first acid treatment step, which lasted 1 hour, leads to dealumination by ≈90% of the final value obtained in the second treatment step (2 hours); after the third step (3 hours) the chemical composition of the obtained product has not changed. All results below refer to samples obtained from a three-stage procedure.

The results for chemical composition of the studied samples, calculated from XR-ED-spectra for 72 oxygen atoms in the unit cell, are given in Table 1 in terms of averaged empirical formulas of dehydrated zeolites; the Si/Al molar ratio shows the degree of dealumination. The degree of decationization is shown in Figure 1 by a decrease in the total charge of all compensating ions, as well as by a change in the proportion of Na^+, K+, Ca^{2+} and Mg^{2+} cations in compensating for the negative charge of the zeolite framework as these cations are leached and replaced in the framework by H^+.

Tab. 1. Chemical composition of original and acid-treated samples

[HCl] [a] (N)	Empirical formula	Si/Al
0	$(Na_{1.96}K_{0.47}Ca_{1.49}Mg_{1.17})[Al_{7.8}Si_{28.2}O_{72}]$	3.6
0.5	$(Na_{0.62}K_{0.67}Ca_{0.71}Mg_{0.47})[Al_{4.59}Si_{31.4}O_{72}]$	6.85
1.0	$(Na_{0.47}K_{0.40}Ca_{0.65}Mg_{0.46})[Al_{4.26}Si_{31.7}O_{72}]$	7.45
2.0	$(Na_{0.096}K_{0.50}Ca_{0.61}Mg_{0.26})[Al_{3.43}Si_{32.6}O_{72}]$	9.5

[a] [HCl] – concentration of hydrochloric acid solution.

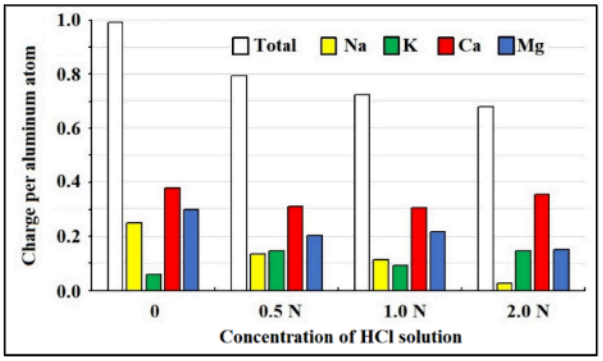

Fig. 1. Charge of cations compensating negative charge of one Al atom in native (0) and acid-treated samples

A decrease in the specific aluminum content and an increase in the Si/Al molar ratio indicates a rather high degree of acid-mediated dealumination; the total charge of metal cations per one aluminum atom monotonically decreases from ≈1 to ≈0.68 with increasing acid concentration. Sodium cations Na^+ ions are washed out to the greatest extent, the content of other cations varies nonmonotonically, but it can be concluded that calcium cations Ca^{2+} are washed out to a lesser extent than magnesium cations Mg^{2+}, while potassium cations K^+ practically do not take part in the decationization process. This conclusion is consistent with the results of the study of decationization and dealumination of Croatian clinoptilolite tuff [9], but do not correspond to the data that the removal of monovalent Na^+ and K^+ cations from Turkish clinoptilolite is insignificant for temperatures of 25-100 °C and changed little with acid concentration [10].

Structure

Powder XRD patterns do not change after treatment of heulandite with dilute HCl solutions with a concentration up to 0.5 N; at a higher concentration, a change in the intensity of some peaks is observed (see Figure 2). In particular, the intensity of the low-angle peak characteristic of heulandite (2Θ = 9.85°, Miller indices *hkl* 020; d-spacing 8.98 Å) decreases, while the intensity of the peaks observed at 2Θ≈22° (*hkl* 131, 400, 330; ≈4 Å) first increases (at 1.0 N), and then decreases (2.0 N), while the intensity of the weak peak at 2Θ≈28° (*hkl* -422 and/or -441; ≈3.15 Å) first decreased, and then sharply increases with increasing acid concentration up to 2N; peaks at 2Θ = 13° (*hkl* -201; 6.8 Å), 15 ° (*hkl* 220; ≈6 Å) and ≈33° (*hkl* -261 and/or 061; ≈2.8 Å) decrease with increasing acid concentration and then disappear from XRD patterns.

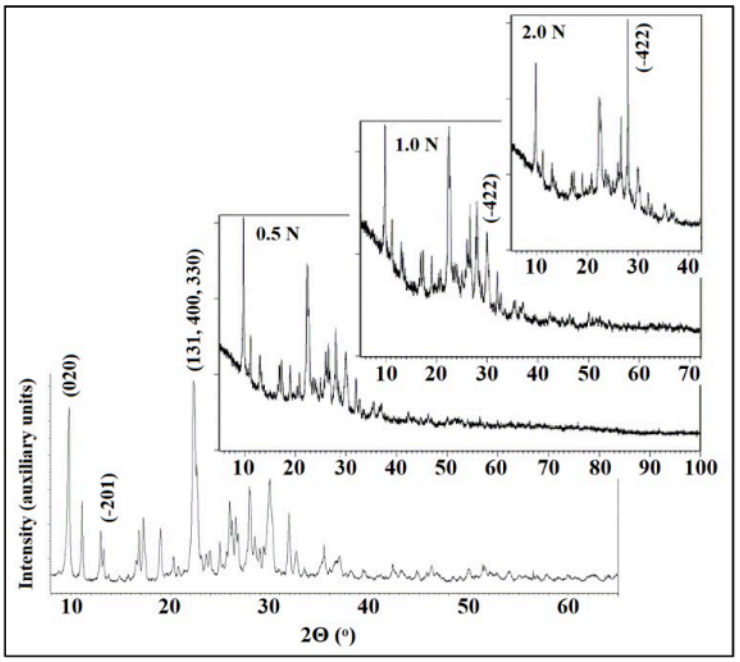

Fig. 2. Powder XRD patterns of original (bottom left) and acid treated samples (numbers in parenthesis are Miller indices hkl).

The overall intensity of the XRD pattern decreases slightly with increasing acid concentration, but there is no peak broadening due to sample amorphization, although acid treatment causes significant dissolution of the sample, which continues in the third stage of treatment, when the amorphization process stops and the chemical composition of the sample ceases to change (see Table 2).

Tab. 2. Weight loss (%) from acid treatment.

	From 0.5 N	From 1.0 N	From 2.0 N
Steps 1-2-3	9.75-7.05-4.5	12.8-7.8-6.1	15.4-7.95-5.25
Total	21.3	26.7	28.6

The result obtained does not contradict the known ones, since in a recent work [7], the amorphization of clinoptilolite recorded using XRD patterns was noted only after treatment of the zeolite with solutions with a high concentration of hydrochloric acid (5 and 10 N).

Sorption of water, benzene and nitrogen

The kinetic diameter of water molecule H_2O is 0.266 nm, and it freely passes through the entrance windows of chabazite and heulandite (see Figure 3).

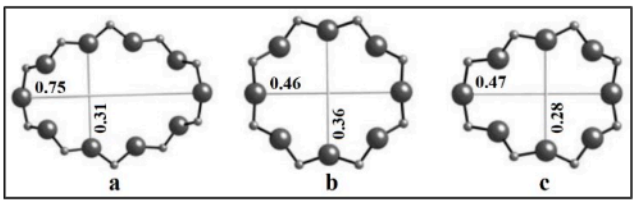

Fig. 3. The entrance windows in heulandite-clinoptilolite according to [11]: 10-membered ring (a) and 8-membered ring (b) viewed along [001], and 8-membered ring (c) viewed along [100]; dimensions are given in nanometers.

The adsorption of small water molecules is a measure of the pore volume of hydrophilic high-aluminum zeolites. Since the filling of micropores occurs at low water vapor pressure, adsorption at a relative pressure of p/p_o=0.4 reflects the micropore volume, and the adsorption capacity at saturated water vapor pressure (p/p_o=1.0) reflects the total volume of all pores [12].

The kinetic diameter of the benzene molecule C_6H_6 (0.585 nm) significantly exceeds the sizes of entrance windows, so that this non-polar molecule can be adsorbed only on the zeolite surface developed due to the presence of meso- and macropores; benzene adsorption capacity also is a relative measure of surface area and its hydrophobicity.

The two entrance windows in the structure of heulandite, 10- and 8-membered rings, are too "narrow" to accommodate a nitrogen molecule N_2 with a kinetic diameter of 0.364 nm, this molecule can hardly pass through only one window, an 8-membered ring with dimensions of 0.46 x 0.36 nm, and this is due to considerable flexibility of heulandite framework [11, pp. 156-157].

Sorption of water and benzene

Results of measurements are shown in Figure 4.

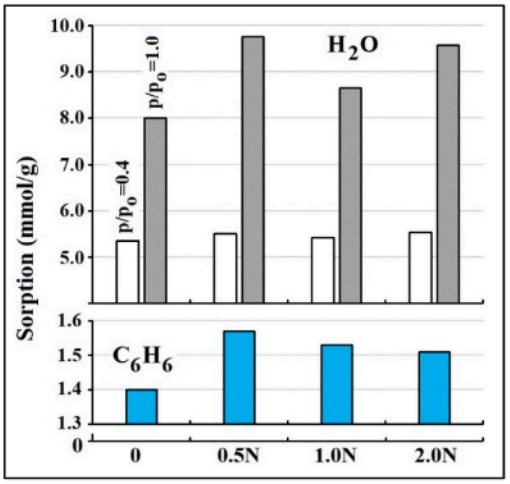

Fig. 4. Adsorption of water vapor (H_2O) and benzene (C_6H_6) on original (0) and acid-treated samples.

The volume of micropores accessible for water molecules for untreated heulandite sample is about 60% of the total pore volume and practically does not change as a result of acid treatment. The adsorption of water vapor in micropores is in no way related to the aluminum content, which is characteristic of high-silica synthetic zeolites [13-15]. The total adsorption in all pores increases nonmonotonically as a result of an increase in the volume of large pores.

Benzene adsorption changes insignificantly, but the results obtained indicate an increase in the hydrophobicity of the surface after acid treatment. More detailed information about surface and mesopores was obtained by analyzing nitrogen adsorption-desorption isotherms.

Nitrogen adsorption

Nitrogen adsorption-desorption isotherms on untreated (0) and acid-treated forms of heulandite are shown in Figure 5, corresponding porosity parameters are given in Table 3.

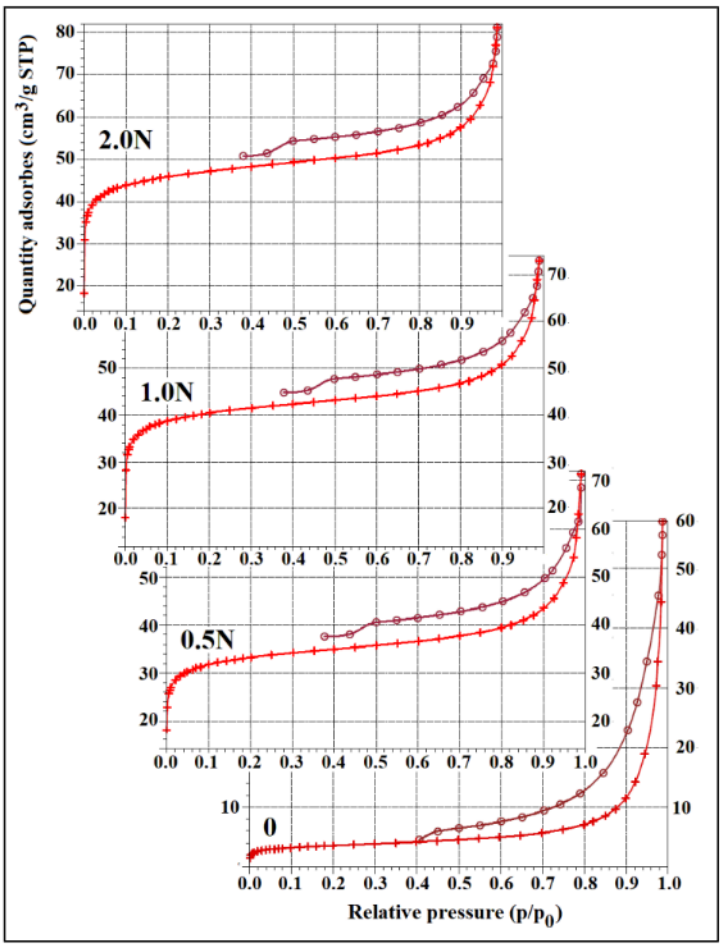

Fig. 5. N_2 adsorption-desorption isotherms on native heulandite (0) and its acid-treated forms.

Tab. 3. Porosity parameters of initial and acid-treated samples.

Concentration of HCl solution (N)	0	0.5	1.0	2.0
BET surface area (m^2/g)	12.8	126.7	154.7	175.0
Total volume of pores (mm^3/g)	89.5	109.0	112.9	125.6
Volume of micropores (mm^3/g)	6.47	78.2	85.6	88.9
BET average pore diameter (nm)	28.0	3.44	2.92	2.87
BJH adsorption/desorption average pore diameter (nm)	38.0	12.1	9.84	9.13
	17.2	13.1	11.6	11.1

The measured isotherms correspond to the filling of micropores (Langmuir plot) at low relative pressures, the BET model well describes the experimental data in the range of relative pressures of $0.01<p/p_o<0.3$ for initial sample and $0.01<p/p_o<0.1$ for acid-treated forms; for all samples a hysteresis loop with a jump at p/p_0= 0.4-0.5 is observed. The initial sample has a low surface area (12.8 m^2/g), and the fraction of micropores accessible to nitrogen molecules is only 7% of the total porosity. Under the influence of acid, the surface area and the volume of micropores accessible to nitrogen molecules increase sharply and continue to increase with increasing acid concentration in the treatment solution. A similar effect was noted in [7] for acid-treated clinoptilolite.

The total pore volume increases monotonically with increasing acid concentration, while the diameters of nanosized pores calculated using the BET and BJH models sharply decrease, indicating that acid treatment affects not only the heulandite micropore system, but also the mesopores existing in its sample. Pore size distribution curve volume vs pore diameter V(D) and differential dV/dD curve calculated by BJH model for initial heulandite and its acid-treated forms are shown in Figure 6.

As the pore size distribution curves V(D) show, the volume of mesopores up to 100 nm in diameter decreases sharply as a result of acid treatment; the concentration of the acid in the treatment solution is not that important. According to the differential curve dV/dD, the maximum at ≈12 nm disappears, but a sharp maximum appears at ≈4 nm. Taking into account, albeit small, but still an increase in the total pore volume with increasing acid concentration, it can be concluded that after acid treatment, small in size, up to 4 nm, pores become predominant in the mesopore system of acid-treated samples.

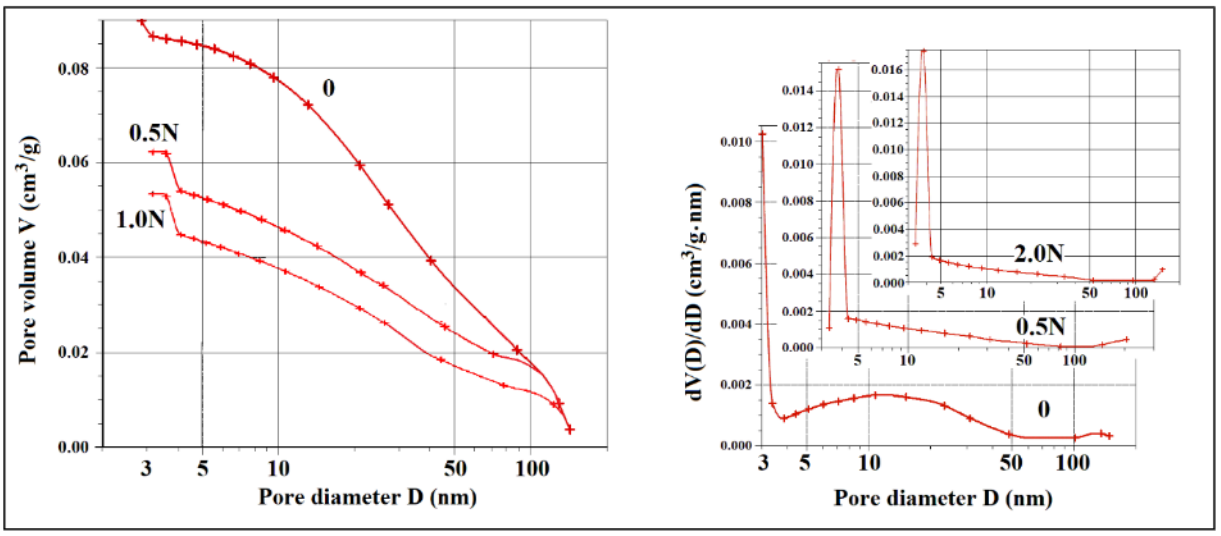

Fig. 6. Pore size distribution V(D) (left) and dV/dD (right) curves calculated by BJH model from desorption isotherms measured on native heulandite (0) and its acid-treated forms.

Ion exchange capacity

The strong dealumination of acid-treated samples limits their use as ion exchangers. Thus, the cation-exchange capacity (CEC), calculated from XR-ED spectral data as the number of milliequivalents of ionogenic groups per gram of the ion exchanger entirely converted to the H^+ form, decreases from 3.03 to 1.9 mEq/g after treatment with a hydrochloric acid solution with a concentration of 0.5 N. However, the "opening" of micropores and the increase in the surface area of the adsorbent occurs abruptly, and a sufficient improvement in the properties of natural zeolite can also be achieved when it is treated with very dilute acid solutions. Table 4 shows the results of measurements (XR-ED) and calculations for samples treated with dilute hydrochloric acid solutions in one step.

Tab. 4. Characteristics and porosity parameters of samples treated witnh diluted HCl solutions.

Concentration of HCl solution (N)	0	0.016	0.032	0.064	0.16	0.32
Si/Al	3.6	3.7	3.7	3.85	4.2	4.8
CEC (mEq/g)	3.03	3.00	2.95	2.90	2.75	2.50
BET surface area (m^2/g)	12.8	15.6	19.6	33.4	49.8	87.5
Total volume of pores (mm^3/g)	89.5	90.0	90.0	92.0	94.0	104
Volume of micropores (mm^3/g)	6.47	10.3	53.2	56.7	63.5	78.2
BET average pore diameter (nm)	28.0	27.0	25.0	22.3	18.6	7.9
BJH adsorption/desorption average pore	38.0	36.2	30.0	28.4	27.1	16.2
diameter (nm)	17.2	17.1	17.0	16.6	16.2	15.4

As the obtained data show, the Si/Al molar ratio as a result of the treatment of heulandite with hydrochloric acid solutions with a concentration of less than 0.1 N changes slightly, and, accordingly, the cation-exchange capacity remains at a fairly high level. The BET surface area and total volume of pores increase, while the average mesopore diameters calculated from the BET and BJH models decrease monotonically with increasing acid concentration, only the micropore volume changes abruptly, increasing sharply after treatment with solutions with a concentration greater than 0.01 N.

Thus, when heulandite is treated with hydrochloric acid solutions with a concentration of 0.01 to 0.1 N, the micropores of the zeolite are "opened" for such large ions as radium Ra^{2+} (diameter 0.324 nm), cesium Cs^+ (0.334 nm), etc. and the zeolite framework still contains a sufficient number of aluminum atoms and, consequently, exchangeable cations.

Conclusion

The effect of acid environment on the heulandite-containing tuff from the Tedzami-Dzegvi deposit leads to significant dealumination and decationization; solutions of hydrochloric acid do not lead to amorphization of the zeolite microporous crystal structure, but gradually dissolve it. The acid treatment also leads to a slight increase in surface hydrophobicity and sharp increase of adsorption in micropores and of the BET surface area, as well as changes in the mesoporous system, leading to the prevalence of pores with a diameter up to 4 nm. Treatment of heulandite with a dilute solution of hydrochloric acid (0.01 – 0.1 N) provides access of large metal ions to the micropores of the zeolite, while maintaining a high ion-exchange capacity.

Acknowledgments

This work was supported by the International Science and Technology Center (ISTC) under the project GE-2506 "Scientific substantiation of the possibility of creating new bactericidal zeolite filter materials for purification-decontamination of water from various sources".

References

1. T. Fisher, A. Dumug, W. Wiehe, " Initial pedogenesii in a topsoil crust 3 years after construction of an artificial catchment in Brandenburg, NE Germany, Biogeochemistry, **101**:165-176 (2010).
2. A. Lukešová, "Soil algae in brown coal and lignite post-mining areas in Central Europe (Czech Republic and Germany) ", Restor Ecol., **9**:341-350 (2001).
3. R. D. Evans, O. L. Lange, "Biological soil crusts and ecosystem nitrogen and carbon dynamics". Ecol Stud., **150**:263-279 (2003).
4. J. Belnap, " Factor influencing nitrogen fixation and nitrogen release in biological soil crusts", Ecol Stud., **150**:241-261(2003).
5. J. L. A. Pluis, "Algal crust formation in the inland dune area, Laarder Wasmeer, the Netherlands", Published By: Springer, **113**:41-51 (1994).
6. O. Rahmonov, J. Piątek, "Sand colonization and initiation of soil development by cyanobacteria and algae". Ekológia (Bratislava), **26**(1):52-63 (2007).
7. I. O. Malam, Y. B. Le, C. Défarge, J. Trichet, "Role of a cyanobacterial cover on structural stability of sandy soils in the Sahelian part of western" Niger, Geoderma, **101**:15-30 (2001).
8. R. Chen, Y. Zhang, Y. Li, W. Wie, J. Zhang, N. Wu, "The variation of morphological features and mineralogical components of biological soil crusts in the Gurbantunggut Desert of Northwestern China". Environ Geol., **57**:1135-1143 (2009).
9. J. R. Johansen, L.E. Shubert, "Algae in soil". Nova Hedwigia, Beih. **123**:297-306 (2001).
10. T. L. Starks, L.E. Shubert, "Colonization and succession of algae and soil algae interactions associated with disturbed areas". J Phycol., **18**:99-107 (1982).
11. J. Belnap, B. Büdel, O. L. Lange, "Biological soil crust: characteristics and distribution". Ecol. Stud., **150**:3-30 (2003).
12. L. S. Khaibullina, N.V. Sukhanova and R.R. Kabirov, "Flora and Syntaxonomy of Soil Algae and Cyanobacteria in Urbanized Areas". Gilem, Ufa, **1**:216 (2011).
13. L. I. Domracheva, E.V. Dabakh, L.V. Kondakova and A.I. Varaksina, "Algal-Mycological Complexes in Soils upon Their Chemical Pollution". Eurasian Soil Science, **39**: 91-97 (2006).
14. L.V. Kuznetsova and D.A. Krivolutskii, "Invertebrate Animals as Environmental Bioindicators in Moscow". Bioindication of the Environmental State in Moscow and Moscow Region, Moscow, pp. 54-57 (1982).
15. V. S. Andrievskii and A. I. Syso, "The Effect of Different Types of Antropogenic Changes in Soils on Communities of Oribatids in Urban Ecosystems". Contemporary Problems of Ecology, **5:**574-579 (2012).
16. O. E. Marfenina, "Anthropogenic Ecology of Soil Fungi". Meditsina Dlya Vsekh, Moscow, pp. 1-195 (2005).
17. V. A. Terekhova, "The Importance of Mycological Studies for Soil Quality Control". Eurasian Soil Science, **40:**583-587 (2007).
18. N. M. Van Straalen and D.A. Krivolutsky, "Bioindicator Systems for Soil Pollution". Kluwer Academic Publishers, Dordrecht, pp. 1-500 (1995).
19. R. R. Kabirov, "Soil Algae of Technogenic Landscapes".Ph.D. thesis, Petersburg University, 1991.
20. R. R. Kabirov and N.V. Sukhanova, "Soil Algae of Urban Lawns", **6**: 175-182 (1997).
21. S. M. Trukhnitskaya and M.V. Chizhevskaya, "Algoflora in the Recreation Areas of the Krasnoyarsk Urboecosystem". KrasGAU, Krasnoyarsk, **1**:135 (2008).
22. L. I. Domracheva, L.V. Kondakova, Y.N. Zykova and V.A. Efremova, "Algal-Cyanomycological Complexes of Urban Soils. In: Ashikhmina, T.Ya. and Domracheva, L.I., Ed., Features of Urboecosystems in the Southern Taiga Subzone of Northeastern Europe", Vyat GGU, Kirov, pp. 120-168 (2012).
23. N. P. Moskvich, "Algological Characterization of the Sanitary State of Soils in Settlements". PhD Disertation, Institute of General and Communal hygiene RAMS, Voroshilovgrad (1972).
24. O. G. Shekhovtsova,. "Soil Algosynusia of Urboecosystems in the Donetsk Azov Region (with Mariupol as an Example) ". Biologicheskii Vestnik Melitopolskogo Gosudarstvennogo Pedagogicheskogo Universiteta im. Bogdana Khmelnitskogo, **3:** 108-118 (2012).
25. O. Shainidze, G. Beridze, A. Murvanidze and G. Chkhubadze, "Macroscopic Algal Growths and Concomitant Micromycetes in the Agrocenosis of Adjara, Georgia", International Journal of Life Sciences Vol. 4. No. 3, pp. 164-167 (2015).
26. O. Shainidze, "Research methods of Autotrophic protists - Algae". Publisher Batumi Shota Rustaveli State University, pp. 3 – 199 (2004).
27. G. Beridze, "Diversity of algoflora of agrocenoses of Adjara". Proceedings of the National Conference, Tbilisi, pp. 79–81 (2011).
28. G. Beridze, "Results of the study of green algae in the agrocenoses of the subtropical zone of Adjara". Academy of Agricultural Sciences of Georgia, **30:** 330-333 (2012).

29. G. Beridze, "Results of studying the algoflora of aquatic plants in small water bodiesAgrocenoses of Adjara". Academy of Agricultural Sciences of Georgia, Tbilisi, **30:** 337-340 (2012).
30. G. Beridze, "Results of a survey of aerophilic algae in agrocenoses of Adjara". Bulletin of the Academy of Agricultural Sciences of Georgia, Tbilisi, **30:** 3-34 (2012).
31. G. Beridze, "Systematic and ecological analysis of cyanophytes in agrocenoses of the subtropical zone of Adjara", Akaki Tsereteli State University. Kutaisi, pp. 115-118 (2012).
32. G. Beridze and O. Shainidze, " Analysis of algoflora of agrocenoses subtropical zone of Adjara", Journal of the National Academy of Sciences of Georgia «Science and Technology, Tbilisi, pp. 16–20 (2012).
33. H. W. Seelay and P.J. Van Demark, "Microbes in Action," A laboratory manual of Microbiology, U. S.A., pp. 1-350 (1981).
34. J. W. G. Lund, "Observation on Soil Algae. 1. The Ecology, Size and Taxonomy of British Soil Diatoms". New Phytologist, 44:196-219 (1945).
35. M. M. Gollerbakh and E.A. Shtina, "Soil Algae". Nauka, Leningrad, pp. 1-228 (1969).
36. G. Gärtner, "Soil Algae. In: Schinner, F., Öhlinger, R., Kandeler, E. and Margesin, R., Ed., Methods in Soil Biology", Springer, Berlin, pp. 295-305 (1969).
37. H. W. Bishoff, and H.C. Bold, "Some Soil Algae from Enchanted Rock and Related Algae Species", University of Texas Publication, **6318:**43-59 (1963).
38. H. Ettl and G. Gärtner, "*Elliptochloris reniformis*". Stuttgart, pp.1-722 (1995).
39. K. Krammer, "Diatoms of Europe", Kommanditgesellschaft, Königstein, pp.1-703 (2000).
40. K. Anagnostidis and J. Komárek, "Modern Approach to the Classification System of Cyanophytes, 3-Oscillatoriales". Algological Studies, **53**:327-472 (1988).
41. S. S. Barinova, L.A. Medvedeva and O.V. Anisimova "Biodiversity of Environmental Indicator Algae". Pilies Studio, Tel Aviv, pp. 3-498 (2006).
42. P. Jaccard, "Distribution de la flore alpine dans le Bassin des Dranses et dans quelques regions voisines". Bulletin de la Société Vaudoise des Sciences Naturelles, **37**: 241-272 (1901).
43. M. F. Dorokhova, N. E. Kosheleva, E. V. Terskaya, "Algae and Cyanobacteria in Soils of Moscow", American Journal of Plant Sciences, **15**: 2461-2471 (2015)